

Bridging Data Islands: Geographic Heterogeneity-Aware Federated Learning for Collaborative Remote Sensing Semantic Segmentation

Jieyi Tan¹, Yansheng Li^{1,*}, Sergey A. Bartalev², Bo Dang¹, Wei Chen¹, Yongjun Zhang¹, Liangqi Yuan³

¹Wuhan University ²Space Research Institute of Russian Academy of Sciences ³Purdue University

tanjieyi@whu.edu.cn yansheng.li@whu.edu.cn

Abstract

Remote sensing semantic segmentation (RSS) is an essential task in Earth Observation missions. Due to data privacy concerns, high-quality remote sensing images with annotations cannot be well shared among institutions, making it difficult to fully utilize RSS data to train a generalized model. Federated Learning (FL), a privacy-preserving collaborative learning technology, is a potential solution. However, the current research on how to effectively apply FL in RSS is still scarce and requires further investigation. Remote sensing images in various institutions often exhibit strong geographical heterogeneity. More specifically, it is reflected in terms of class-distribution heterogeneity and object-appearance heterogeneity. Unfortunately, most existing FL studies show inadequate focus on geographical heterogeneity, thus leading to performance degradation in the global model. Considering the aforementioned issues, we propose a novel **Geographic Heterogeneity-Aware Federated Learning (GeoFed)** framework to address privacy-preserving RSS. Through *Global Feature Extension and Tail Regeneration* modules, class-distribution heterogeneity is alleviated. Additionally, we design an *Essential Feature Mining* strategy to alleviate object-appearance heterogeneity by constructing essential features. Extensive experiments on three datasets (i.e., *FBP*, *CASID*, *Inria*) show that our *GeoFed* consistently outperforms the current state-of-the-art methods. The code will be available publicly.

1. Introduction

Remote sensing semantic segmentation (RSS) is a prevalent solution in the automatic land use and land cover mapping (LULC) [10, 35, 37, 52]. It requires a large amount of dense and diverse annotations to train deep models in large-scale scenarios. However, high-quality remote sensing images with annotations tend to be distributed across institutions, thus data sharing is still hindered by geospatial information security and industry competitions [43]. In the con-

*Corresponding author.

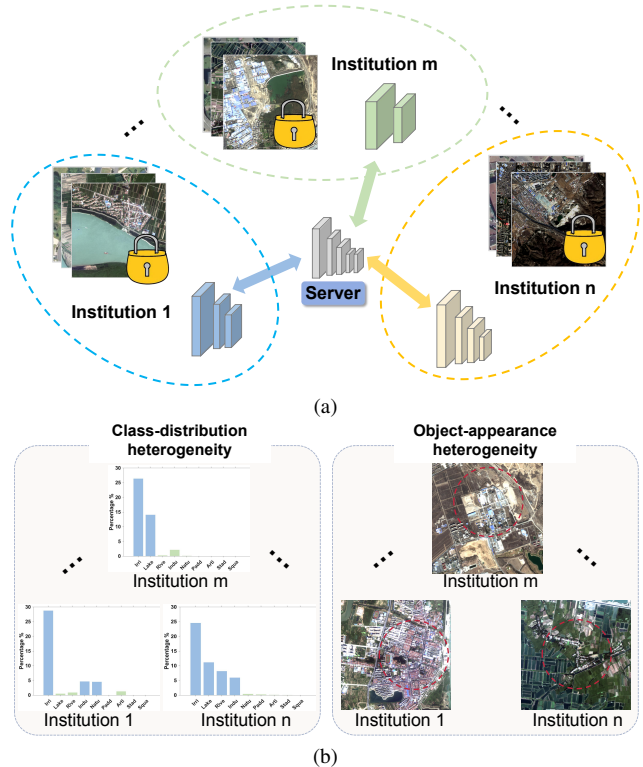


Figure 1. (a) Illustration of FL for RSS. Institutions only transmit model parameters, without disclosing their private data, therefore achieving privacy-preserving collaborative learning. (b) Traditional FL applied in RSS encounters geographic heterogeneity. The coexistence of class-distribution heterogeneity and object-appearance heterogeneity limits the global model performance.

text of data islands, local data on the islands face the challenge of scarcity. Federated learning (FL) is a decentralized paradigm to train a generalized global model. In FL, each institution only needs to train and exchange models locally without sharing its private data, thus pursuing the approximation of centralized learning on large-scale data [25, 44]. Hence, FL is promising to address the challenges of remote sensing data islands but is scarcely explored in RSS.

As the second law of geography says, *geographic vari-*

ables exhibit uncontrolled variance [12]. The formation of geographical landscapes is a complex interplay of various factors, such as climate, geology, hydrology, biodiversity, and human activities. These factors contribute to shaping the unique characteristics of different regions [30, 51]. Remote sensing data from various institutions are typically collected from different regions, resulting in geographic heterogeneity among institutions. Therefore, when optimizing locally, each institution tends to focus on its own local optimum, which is inconsistent with the direction of the global model constructed through FL, making it difficult for the FL model to converge to the global optimum. In Fig. 1, we present the application of FL in RSS and the challenges brought about by geographic heterogeneity. Recently, lots of studies [3, 19, 26, 27] are dedicated to addressing the issue of heterogeneity. However, the existing research on the effective application of FL in RSS remains insufficient and calls for further investigation. Therefore, the advantages of FL in RSS are not well demonstrated. Most of the works do not fully take into account the data characteristics in RSS. From a more comprehensive perspective, there exists both class-distribution heterogeneity and object-appearance heterogeneity in the RSS data among the institutions. A detailed explanation of how these two types of heterogeneity are reflected in RSS is as follows:

Class-distribution heterogeneity: As is shown in the left part of Fig. 1b, each local dataset grapples with a class imbalance problem. Moreover, local class distributions vary and do not align with the global class distribution. Additionally, class imbalance in remote sensing images typically presents as a long-tailed distribution [49]. In extreme cases, some institution datasets may lack certain classes. This situation intensifies the problem of class imbalance, especially for minority class samples [10, 20]. (For example, due to a combination of various regional factors, the number of common geographical features significantly outnumbers uncommon ones. institutions in tropical regions may have an abundance of forests but little to no snow. Conversely, polar regions may have more snow. From a global perspective, snow then becomes a minority category.)

Object-appearance heterogeneity: In the right part of Fig. 1b, different regions have different characteristics for the same land cover category, which becomes more evident in coarse-grained classification systems [14, 36, 37, 52]. For example, in rainy areas, there is a tendency to construct houses with pointed roofs for better drainage compared to dry areas. As a result, the overall feature representations of the buildings differ across different institutions. The global model needs to learn the essential features (*e.g.* regular shape of buildings) while also maintaining robustness to diverse institution-specific features (*e.g.* flat or pointed roofs) [45]. The complexity increases further as geographic heterogeneity is often characterized by the coexistence of

class-distribution heterogeneity and object-appearance heterogeneity.

Considering the aforementioned challenges, we propose a **Geographic Heterogeneity-Aware Federated Learning** (GeoFed) framework to formulate a novel paradigm for privacy-preserving collaborative RSS. Through Global Feature Extension (GFE) and Tail Regeneration (TR) modules, class-distribution heterogeneity is alleviated. Additionally, we design an Essential Feature Mining (EFM) strategy to alleviate object-appearance heterogeneity by constructing essential features. Our main contributions are summarized as follows:

- We propose a novel privacy-preserving RSS framework by geographic heterogeneity-aware federated learning, which is a general framework that can support both CNN and Transformer.
- This paper comprehensively considers RSS-oriented geographic heterogeneity in privacy-preserving learning. We propose GFE and TR to alleviate class-distribution heterogeneity. An EFM strategy is proposed to alleviate object-appearance heterogeneity.
- Extensive experiments on three public datasets (*i.e.*, FBP, CASID, Inria) with typical geographical heterogeneity show our GeoFed framework outperforms state-of-the-art methods on three datasets, simultaneously.

2. Related Work

2.1. Federated Learning

The pioneering FedAvg [25] trains a global model by aggregating local model parameters. In each communication round, all institutions receive the aggregated model parameters and conduct the *Local Update* procedure in parallel. Subsequently, the server aggregates the optimized model parameters from institutions into a single model which is used in the next communication round.

However, in scenarios with heterogeneous data, its performance will significantly decrease [3, 18, 31, 45]. Recently, many studies have proposed methods to deal with this challenge from different perspectives. FedSeg [27] proposes a framework to address the class heterogeneity in FSS, but it focuses more on addressing the foreground-background inconsistency problem, which is not a key issue in remote sensing semantic segmentation. FISS [9] studies how to achieve incremental learning in federated semantic segmentation, with a particular focus on addressing the catastrophic forgetting issue caused by heterogeneous data. Some other methods adopt strategies from domain generalization [11, 15, 21, 38]. GBME [46] designs a proxy as the class prior for re-balancing algorithms without requiring additional private information, but it can not be applied to the more challenging semantic segmentation task. Some studies utilize prototype learning to solve the prob-

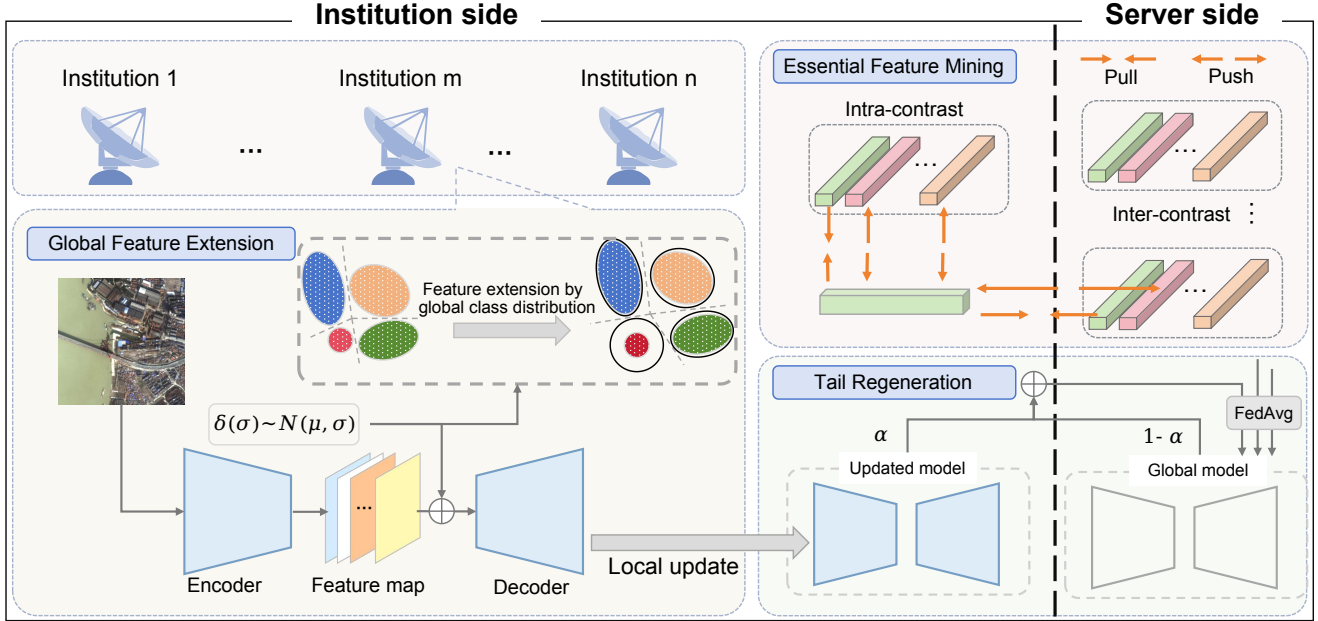


Figure 2. An overview of our proposed GeoFed framework. It mainly contains three components as shown in the figure. Firstly, class-distribution heterogeneity is alleviated through the utilization of the Global Feature Extension and Tail Regeneration modules. GFE expands the feature diversity of local models under the global class distribution, and TR restores the knowledge of the global model on all classes. Next, an Essential Feature Mining strategy containing intra & inter contrastive loss is applied to alleviate object-appearance heterogeneity.

lem [16, 28]. Some studies investigate the architecture of federated models, and observe that heterogeneity can be alleviated by Transformers [5, 29]. Moreover, Some other works focus on the aggregation procedures. Elastic aggregation [4] reduces the magnitudes of updates to the more sensitive parameters to prevent the server model from drifting to any one institution distribution, and conversely boosts updates to the less sensitive parameters to better explore different institution distributions.

Most of the aforementioned works do not fully take into account the data characteristics in RSS.

2.2. Privacy-Preserving RS Interpretation

Remote sensing interpretation requires a large amount of sensitive geospatial data. Privacy protection in remote sensing interpretation has gradually brought attention along with the application of deep learning techniques [43].

In literature, some pioneering studies build FL frameworks on Unmanned Aerial Vehicle (UAV) swarms, which enables different devices to collaboratively monitor without sharing raw data [7, 23, 50]. SACDF [2] proposes an improved FL for the hyperspectral classification task, using the multidimensional spatial details of hyperspectral images to perceive decision boundaries. Some studies explore the application of FL in remote sensing image classification [33, 34], but these methods consider classification tasks rather than the more challenging semantic segmentation tasks. Some recent studies validate FL on RSS datasets,

but they neglect the geographical heterogeneity of remote sensing images [17, 47, 48]. FedPM [48] proposes an FL method based on prototype matching for object extraction in remote sensing, but it does not consider the problem of multi-class segmentation and ignores the class-distribution heterogeneity in RSS.

Different from these existing privacy-preserving RS interpretation works, our GeoFed framework demonstrates a strong awareness of geographical heterogeneity, enabling effective improvement in collaborative RSS performance.

3. Method

3.1. Preliminaries

Suppose there are a total of n institutions participating in FL, and the i -th institution has its private RSS dataset $\mathcal{D}^i: \{x_m^i, y_m^i\}_{m=1}^{|\mathcal{D}^i|}$. Each pixel x_m^i has a corresponding class label y_m^i . The entire dataset can be expressed as $\mathcal{D} = \{\mathcal{D}^1, \mathcal{D}^2, \dots, \mathcal{D}^n\}$. Assume there are a total of C categories in the dataset, and let f_c^i denote the label frequency of class c in the i -th institution.

In the traditional paradigm, the whole dataset \mathcal{D} is directly utilized to conduct centralized training. In the FL paradigm, our goal is for each institution to train a semantic segmentation model w with good generalization without transferring the local dataset \mathcal{D}^i . The loss function can be formulated:

$$\arg \min_w \mathcal{L}(w) = \sum_{i=1}^n \frac{|\mathcal{D}^i|}{|\mathcal{D}|} \mathcal{L}_i(w), \quad (1)$$

where $|\mathcal{D}|$ denotes the number of samples in \mathcal{D} , $\mathcal{L}_i(w)$ denotes the empirical loss of institution i :

$$\mathcal{L}_i(w) = \mathbb{E}_{(\mathbf{x}, \mathbf{y}) \in \mathcal{D}^i} \ell_i[(\mathbf{x}, \mathbf{y}); w], \quad (2)$$

where ℓ_i is the local loss of the model w in institution i for the satellite image \mathbf{x} and its corresponding mask \mathbf{y} in the local dataset \mathcal{D}^i .

The data distribution of the i -th institution is denoted as $P_i(x, y)$ which can be rewritten as $P_i(x|y)P_i(y)$. For class-distribution heterogeneity, $P_{i_1}(y) \neq P_{i_2}(y)$ ($i_1 \neq i_2$), in extreme cases, some institutions may lack categories. For object-appearance heterogeneity, $P_{i_1}(x|y) \neq P_{i_2}(x|y)$ ($i_1 \neq i_2$), this means that objects of the same category present different appearance in different institutions.

3.2. Overview

An overview of our GeoFed is presented in Fig. 2. To alleviate the issue of class-distribution heterogeneity, we propose the Global Feature Extension module (Sec. 3.3), which enables institutions to learn more diverse features and aligns them with the global class distribution, thus mitigating class imbalance. We propose a Tail Regeneration strategy (Sec. 3.4), analogous to the anti-forgetting mechanism, which effectively integrates the knowledge of a more knowledgeable global model and an institution model, mitigating the performance degradation of some classes caused by class-distribution heterogeneity. To address the problem of object-appearance heterogeneity, we propose the Essential Feature Mining strategy (Sec. 3.5), which utilizes contrastive loss to facilitate the learning of more compact and discriminative features by institution models and encourages the discovery of common essential features across institutions. These modules will be elaborated in detail in the following sections.

The total objective for the proposed GeoFed framework is written as follows:

$$\mathcal{L} = \mathcal{L}_{CE} + \lambda_1 \mathcal{L}_{inter} + \lambda_2 \mathcal{L}_{intra}, \quad (3)$$

where \mathcal{L}_{CE} is from the the Global Feature Extension module. The details of \mathcal{L}_{inter} and \mathcal{L}_{intra} will be elaborated in the Essential Feature Mining strategy. Moreover, λ_1 and λ_2 are hyper-parameters used to control the weights of the inter-contrastive loss and intra-contrastive loss. The Tail Regeneration module does not involve optimizing the loss function.

3.3. Global Feature Extension

Classes with fewer labels often lack robust feature representations due to the insufficient sample size. On the insti-

Algorithm 1: Our GeoFed framework

Input : Total number of institutions n , total number of communication rounds T , local learning rate η , local training epoch E

Output: global RSS model ω .

- 1 **Initialization**: Randomly initialize the global model ω .
- 2 **Local Update**:
- 3 **for** $E = 0$ **to** $E - 1$ **do**
- 4 Download global model ω
- 5 Calculate local class frequency Eq. (4)
- 6 Global $f_c \leftarrow \text{MPC}()$
- 7 $\mathcal{L}_{CE} \leftarrow$ Perturbations. Eq. (5)
- 8 Online essential feature update. Eqs. (10) and (11)
- 9 $\mathcal{L}_{intra}, \mathcal{L}_{intra} \leftarrow$ Contrastive Eqs. (12) and (13)
- 10 $\mathcal{L} = \mathcal{L}_{CE} + \lambda_1 \mathcal{L}_{inter} + \lambda_2 \mathcal{L}_{intra}$ Eq. (3)
- 11 Tail Regeneration. Eq. (8)
- 12 **end**
- 13 **Server Execution**:
- 14 **for** $t = 0$ **to** $T - 1$ **do**
- 15 Distribute the current global model ω to each institution.
- 16 **for** institution $i = 1$ **to** m **in parallel do**
- 17 Updated model $\omega_i^t \leftarrow \text{LocalUpdate}(i, \omega)$
- 18 Essential features $\leftarrow \text{LocalUpdate}(i, \omega)$
- 19 **end**
- 20 $\omega = \sum_{i=1}^n \frac{|\mathcal{D}^i|}{|\mathcal{D}|} \omega_i^t$
- 21 **end**

tutional side, we propose diversity enhancement for global tail categories. Firstly, we calculate the class frequency vector of each institution using the following formula:

$$f_c = \frac{\sum_{i=1}^N \sum_{j=1}^{H \times W} y^{i,j,c}}{N \times H \times W}, \quad (4)$$

where N , W , H denote the number of batches, width, and height of the image, respectively. The global class frequency f_c can be obtained by calculating the local frequency vectors of each institution.

Each pixel corresponds to a feature vector q_i and a true class label y_i^c . We assign smaller Gaussian perturbations to head categories and larger Gaussian perturbations to tail categories. The formula is as follows:

$$q_i' = q_i + w_c |\delta(\sigma)|, \quad (5)$$

where $\delta(\sigma)$ follows a Gaussian distribution with mean 0 and standard deviation σ . We denote $f_{c'} = \frac{1}{f_c + \epsilon}$, ϵ is for ensure not divided by zero. w_c is the perturbation scale, and is normalized by Eq. (6):

$$w_c = \frac{e^{f_{c'}}}{\sum_{c=1}^C e^{f_{c'}}}. \quad (6)$$

The loss is computed using the conventional Cross-Entropy loss on the feature map after applying Gaussian

perturbations, as shown in Eq. (7),

$$\mathcal{L}_{CE} = - \sum_{c=1}^C y_c^i \log p^i. \quad (7)$$

It is worth noting that privacy leakage of local class distribution is not a concern here, as the global frequency vector can be easily obtained without leaking local frequency vector information using Secure Multi-party Computation (MPC) technology [1].

3.4. Tail Regeneration

The most extreme manifestation of the long-tail distribution is the phenomenon of ‘‘Broken Tail’’, where some institutions experience category absence, thereby exacerbating the issue of class imbalance. For a given institution m , we regard categories with a total pixel percentage less than τ as ‘‘Broken Tail’’. The number of remaining categories is signified as $M_{residue}$.

Drawing inspiration from EWF [40], we design a simple yet efficient Tail Regeneration (TR) strategy to combat the issue of ‘‘Broken Tail’’. For every aggregated global model (θ_{global}), the model becomes more experienced via the process of aggregation and generally possesses a better recognition ability for each category. The updated model (θ_{update}) post-local training at the institution’s end tends to overfit the remaining categories. We introduce the parameter α to preserve the original global model’s insights. The TR strategy can be expressed as

$$\theta_{TR} = \alpha \theta_{update} + (1 - \alpha) \theta_{global}, \quad (8)$$

where α is defined as follows:

$$\alpha = \sqrt{\frac{C_{residue}}{C + C_{residue}}}. \quad (9)$$

3.5. Essential Feature Mining

The essential feature of the category c in the i -th institution is obtained using masked average pooling [32] based on the representation of pixel j , denoted as $P_i(j)$.

$$p_{c,i}^t = \frac{\sum_j P_i(j) \mathbb{1}[y_i(j) = c]}{\sum_j \mathbb{1}[y_i(j) = c]}, \quad (10)$$

where $\mathbb{1}$ is the indicator function, and t is the number of communication round. The essential features $p_{c,i}^t$ are updated online and initialized as a vector following the Gaussian distribution of $\mathcal{N}(0,1)$. The formula for online updating is as follows:

$$p_{c,i}^t = \gamma p_{c,i}^{t-1} + (1 - \gamma) p_{c,i}^{t-1} \quad (11)$$

To better explore essential features and promote the model to learn common features, we design intra-contrastive loss and inter-contrastive loss.

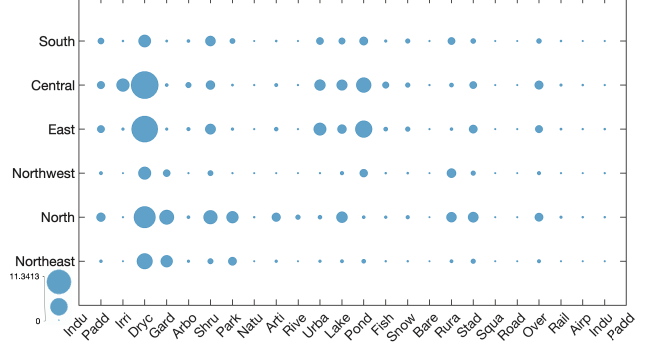


Figure 3. Visualization of the heterogeneous class distribution in the FBP dataset. The larger the bubble size, the greater the proportion of pixels corresponding to that class in the institution.

For intra-contrastive loss, the objective is to promote the proximity of feature representations belonging to the same categories within each institution, fostering a cohesive grouping. Simultaneously, the loss seeks to maximize the separation between feature representations corresponding to distinct categories, emphasizing distinctiveness.

$$\mathcal{L}_{intra} = \sum -\log \frac{\exp(p_j p_{c+} / \tau)}{\exp(p_j p_{c+} / \tau) + \sum_{p_{c-}} \exp(p_j p_{c-} / \tau)}, \quad (12)$$

For inter-contrastive loss, we aim to make the pixel feature representations of a certain category in one institution close to the essential features of the same category in other institutions, while being far from the essential features of different categories in other institutions. This enables each institution to optimize towards the global essential features and alleviates the issue of object-appearance heterogeneity.

$$\mathcal{L}_{inter} = \frac{1}{n} \sum_{i=1}^n -\log \frac{\exp(p_j^i p_{c+} / \tau)}{\exp(p_j^i p_{c+} / \tau) + \sum_{p_{c-}} \exp(p_j^i p_{c-} / \tau)}, \quad (13)$$

where p_j^i denotes the normalized representation vector of a sample pixel in the i -th institution. p_{c+} denotes the essential feature of the same class, and p_{c-} is of the different classes. τ is the temperature parameter.

The overall algorithm of our GeoFed framework is shown in Algorithm 1.

4. Experiments

4.1. Experimental Setup

Datasets. We conduct experiments on three public datasets to validate our framework. They are FBP [37], CASID [22] and Inria [24]. FBP is annotated according to a 24-category system and contains a total of 150 satellite images from China with a size of 6800×7200 pixels. Based on the geographical divisions of China, we divide the dataset into six regions (*i.e.*, Northeast, North, Northwest, Central, East,

		Centralized	Solo	FedAvg[25]	FedProx[19]	FedSM[42]	FedReF[31]	Elastic[4]	GeoFed(Ours)
FBP	Northeast	73.82	66.62	66.62	64.91	67.57	62.21	68.42	69.02
	North	66.30	59.74	58.62	57.28	60.34	58.12	62.34	62.20
	Northwest	66.92	63.43	60.11	61.33	63.20	60.17	64.32	65.21
	East	71.09	66.50	65.82	65.19	66.34	61.33	68.10	68.89
	Central	68.61	66.68	64.95	64.68	67.21	65.21	67.43	68.11
	South	72.28	61.01	62.08	61.59	66.54	61.98	65.33	65.78
	Average	69.84	64.00	63.03	62.50	65.20	61.50	65.99	66.54
CASID	TemMs	48.56	41.33	44.54	43.17	45.63	43.15	45.48	46.33
	SubMs	65.89	59.12	62.66	62.48	63.43	62.87	64.26	63.30
	TroMs	62.54	57.27	58.47	58.80	59.52	56.98	60.54	61.27
	TroRf	56.01	49.54	51.08	50.21	51.07	50.97	51.25	52.11
	Average	58.25	51.82	54.19	53.67	54.91	53.49	55.38	55.75
Inria	Austin	57.51	53.14	55.27	54.42	55.10	55.39	56.14	56.32
	Chicago	48.06	45.69	46.56	46.87	47.00	46.13	47.71	47.74
	Kitsap	49.18	39.90	44.42	43.17	44.55	45.22	47.64	48.08
	West Tyrol	57.60	51.16	54.76	54.92	54.12	51.73	55.27	55.41
	Vienna	56.37	49.37	53.88	54.17	50.18	51.42	54.70	54.86
	Average	53.74	47.85	50.98	50.71	50.19	49.98	52.29	52.49

Table 1. Comparisons with previous SOTA Methods under the mIoU (%) metric on three datasets. Each row represents the performance of various methods in the corresponding institution test set of that row. The best results are marked in **bold**. The same applies to the subsequent tables.

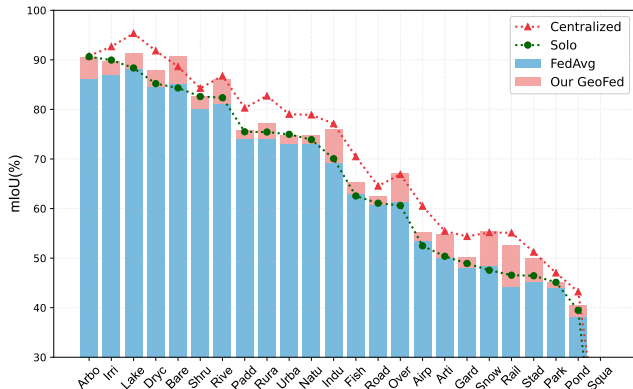


Figure 4. Comparison of Centralized, Solo, FedAvg and our GeoFed for each class.

and South). We present the severe class-distribution heterogeneity in Fig. 3. CASID contains a total of 980 images with a size of 5000×5000 pixels, from four typical climatic zones (*i.e.*, temperate monsoon, subtropical monsoon, tropical monsoon, and tropical rainforest). Due to climate being an important factor in land cover features, there is a high geographic heterogeneity among the four institutions. Inria is an aerial image dataset for building extraction. It contains 180 images of size 5000×5000 pixels. The data is divided into five different cities (*i.e.*, Austin, Chicago, Kitsap, West Tyrol, and Vienna), with significant heterogeneity in architectural styles between institutions.

Evaluation metrics. The mean intersection-over-union (mIoU) metric is adopted to evaluate the segmentation per-

formance of the FBP and CASID datasets. Additionally, for the Inria dataset, the IoU metric is utilized for performance evaluation.

Implementation details. The experiments simulate the FL process with PyTorch using a single NVIDIA RTX Titan GPU with 24-GB GPU memory in a serial manner. Due to memory limitations, all images are cropped to patches with a size of 512×512 pixels. Unless otherwise specified, all experiments use DeepLabv3+ [6] as the segmentation model. The ResNet-50 [13] pretrained on ImageNet[8] is used as the backbone. The optimizer is SGD with an initial learning rate of 0.001 and the batch size is set to 4. We employ a poly learning rate scheduler. The server performs 100 aggregation operations to ensure convergence, and local institutions update themselves with 1 epoch. In the experiments, we set λ_1 and λ_2 as 0.4 and 0.6. The temperature τ is set as 0.05. The update ratio of essential features γ is set as 0.8.

4.2. Comparison with State-of-the-arts

In this section, we compare our method with previous SOTA methods focusing on addressing data heterogeneity issues: FedProx[19], FedSM[42], FedReF[31], Elastic[4]. FedAvg serves as the baseline method for the experiments. We report the zone-wise performance of our method and other methods in Tab. 1.

Solo refers to a scenario where each institution trains its model solely using its local private data and evaluates the model locally. This approach is akin to the method men-

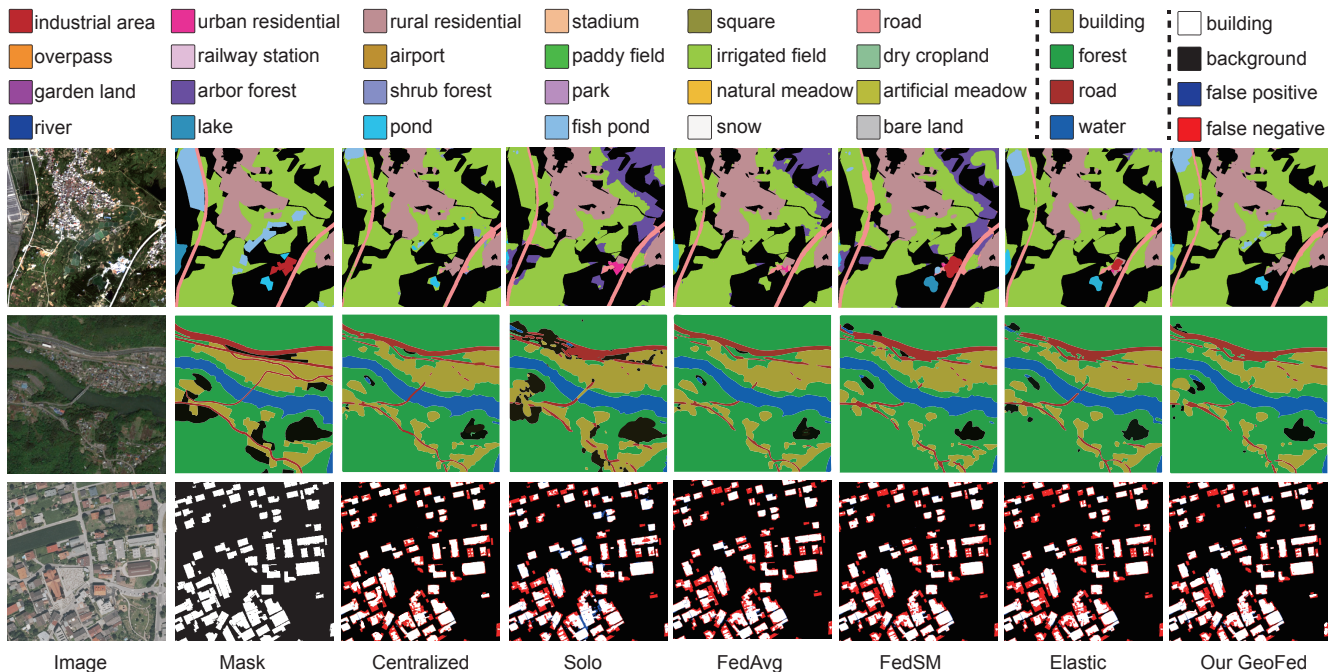


Figure 5. Visualization of the comparison among SOTA methods. The first line shows the results on FBP, the second line shows the results on CASID, and the third line shows the results on the Inria dataset. Best viewed in colors.

tioned in Sec. 2, where each institution independently trains its model and produces local maps, eventually merging all results to obtain a large-scale remote sensing semantic segmentation map. Centralized refers to aggregating all data together and training on the entire dataset. It should be noted that this approach violates data privacy assumptions. However, it can be anticipated that this provides a potential performance upper limit reference for FL. Our goal is to approach or even surpass this reference as closely as possible.

We observe that our proposed GeoFed framework achieves state-of-the-art performance on three datasets and is very close to the results of centralized training. Our method surpasses the Solo method by 2.54%, 3.93%, and 4.64% on the three datasets, respectively, demonstrating the advantages of FL over partition-based mapping and the effective aggregation of knowledge from different regions. Additionally, the gaps between our method and the Centralized method are 3.30%, 2.50%, and 1.25% on the three datasets, respectively. Due to the geographic heterogeneity issues in the FBP and CASID datasets, which involve multi-class semantic segmentation, the challenge posed is more severe compared to Inria, resulting in larger gaps.

On the FBP dataset, our method outperforms the baseline method FedAvg by 3.51%, confirming the effectiveness of our geographic heterogeneity-aware method in alleviating performance loss caused by heterogeneous data. Furthermore, our method surpasses the previous state-of-the-art method Elastic by 0.55%. It’s worth noting that in the experimental results, FedAvg, FedProx, and FedReF were

Test \ Train	NE	N	NW	E	C	S	Avg
NE	<u>66.62</u>	32.73	40.52	48.72	41.51	31.74	43.64
N	39.32	<u>59.74</u>	31.43	35.89	40.89	31.92	39.87
NW	39.83	38.32	<u>63.43</u>	41.36	39.71	39.24	43.65
E	44.54	34.77	42.58	<u>66.50</u>	41.54	36.76	44.45
C	42.91	39.49	35.05	40.40	<u>66.68</u>	29.55	42.35
S	37.05	38.40	42.29	42.80	37.84	<u>61.01</u>	43.23
GeoFed	69.02	62.20	65.21	68.89	68.11	65.78	66.54

Table 2. Cross-domain test results for the performance of the six regions (Northeast(NE), North(N), Northwest(NW), Central(C), East(E), South(S)) in FBP. The results underlined correspond to the Solo method in Tab.1

unable to surpass the Solo method. In the context of geographic heterogeneity, these methods fail to learn the consistency between categories. The iterative aggregation process actually undermines the capability of the model. FedProx, in particular, performs worse than the baseline method FedAvg on all three datasets, indicating that simple model parameter constraints cannot effectively address the heterogeneity issues in all scenarios, especially in semantic segmentation where model parameters tend to be larger.

On the CASID dataset, our method outperforms the previous state-of-the-art method Elastic by 0.37%. On the Inria dataset, we find that our method achieves stable performance improvements in every city. Some cities(*e.g.* Kit-sap) with poor performance in individual training, achieve

Method	GFE	TR	EFM	mIoU(%)	Δ (%)
Baseline				63.03	
I	✓			64.55	+1.52
II		✓		64.49	+1.46
III			✓	64.70	+1.67
IV	✓	✓		65.14	+2.11
V	✓		✓	65.51	+2.48
VI		✓	✓	65.89	+2.86
VII	✓	✓	✓	66.54	+3.51

Table 3. Ablation study of the key components in our framework.

a significant performance improvement of 8.18% through our method.

In Fig. 4, we illustrate the IoU performance of classes for several methods, including Centralized, Solo, FedAvg, and Our GeoFed. Our approach achieves performance improvements on almost every class, especially some tail classes, and approaches the performance of the ideal Centralized method.

Tab. 2 presents the results of different institutions using private datasets for local model training and testing on other test sets. It can be seen that the geographical heterogeneity of different institutions leads to a severe domain gap, resulting in poor generalization performance of the models. However, our GeoFed framework effectively enables communication among individual models and achieves a good balance between erudite and expertise. Compared to each locally trained model, which performs well in its own domain, overall performance is improved by an average of over 20%. GeoFed successfully alleviates overfitting in each local model.

4.3. Empirical Analysis

Effectiveness of the proposed components: In Tab. 3, we conducted ablation experiments. We used FedAvg as the baseline method, where the GFE, EFM, and TR modules were used individually, resulting in mIoU improvements of 1.52%, 1.67%, and 1.46% respectively. This demonstrates the effectiveness of our proposed method in addressing heterogeneity issues. When all the modules proposed by us were added to the baseline, our GeoFed achieved a performance improvement of 3.51%.

Different models: Our proposed method is applicable to mainstream semantic segmentation models. To further validate the robustness of our method, we conducted experiments using different models in the context of FL in Tab. 4. Between the HRNet-W48 and SegFormer-B2 models, our method benefits from stronger feature extraction backbones, resulting in performance improvements of 1.74% and 3.04% respectively.

Visualization: In Fig. 5, we visualize the final semantic segmentation results of different methods. From the figure,

Method	HRNet-W48 [39]	SegFormer-B2 [41]
FedAvg [25]	67.57	67.31
FedProx [19]	67.12	67.84
FedSM [42]	67.86	68.55
FedReF [31]	66.94	67.37
Elastic [4]	68.01	69.11
Our GeoFed	68.28	69.58

Table 4. Results of different institution models.

it can be observed that our method provides clearer boundaries in the segmentation. Additionally, our GeoFed has fewer misclassification results, indicating that through the several modules proposed by us, the model has improved learning for classes with fewer samples. Moreover, by effectively aggregating knowledge from various institutions devices, it promotes semantic consistency among classes. As is shown in Fig. 6, we present the t-SNE plots of our method and FedAvg’s hidden layer features. It is evident that our method achieves more compact features within the same class and obtains greater inter-class separability.

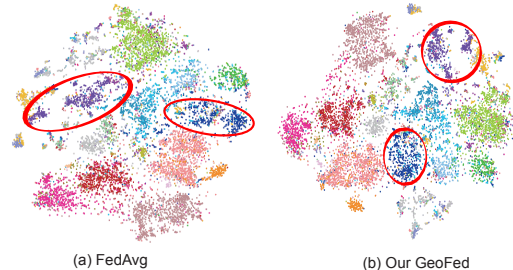


Figure 6. t-SNE visualization of the pixel-level features generated by FedAvg (a) and our GeoFed (b)

5. Conclusion and Future work

This paper proposes a novel GeoFed framework. GeoFed is a general framework that includes multiple meticulously designed modules to address the geographic heterogeneity. These modules are interconnected and optimized together under a overall loss function. More specifically, Global Feature Extension aligns the local class distribution with the global class distribution. Tail Regeneration restores the recognition ability of tail classes, thus class-distribution heterogeneity is alleviated. The Essential Feature Mining strategy is applied to alleviate object-appearance heterogeneity by using inter and intra-contrastive loss. Extensive experiments on three datasets show that our GeoFed consistently outperforms the current state-of-the-art methods.

We hope the release of our code will inspire further research on privacy-preserving collaborative learning in remote sensing. Our future work aims to investigate the potential performance improvement of FL models benefiting from LULC zoning mapping.

References

- [1] David Byrd and Antigoni Polychroniadou. Differentially private secure multi-party computation for federated learning in financial applications. In *Proceedings of the First ACM International Conference on AI in Finance*, pages 1–9, 2020. 5
- [2] Weiwei Cai, Ming Gao, Yao Ding, Xin Ning, Xiao Bai, and Pengjiang Qian. Stereo attention cross-decoupling fusion-guided federated neural learning for hyperspectral image classification. *IEEE Transactions on Geoscience and Remote Sensing*, 61:1–16, 2023. 3
- [3] Debora Caldarola, Barbara Caputo, and Marco Ciccone. Improving generalization in federated learning by seeking flat minima. In *European Conference on Computer Vision*, pages 654–672. Springer, 2022. 2
- [4] Dengsheng Chen, Jie Hu, Vince Junkai Tan, Xiaoming Wei, and Enhua Wu. Elastic aggregation for federated optimization. In *Proceedings of the IEEE/CVF Conference on Computer Vision and Pattern Recognition (CVPR)*, pages 12187–12197, 2023. 3, 6, 8
- [5] Haokun Chen, Ahmed Frikha, Denis Krompass, Jindong Gu, and Volker Tresp. Fraud: Tackling federated learning with non-iid features via representation augmentation. In *Proceedings of the IEEE/CVF International Conference on Computer Vision (ICCV)*, pages 4849–4859, 2023. 3
- [6] Liang-Chieh Chen, Yukun Zhu, George Papandreou, Florian Schroff, and Hartwig Adam. Encoder-decoder with atrous separable convolution for semantic image segmentation. In *Proceedings of the European Conference on Computer Vision (ECCV)*, 2018. 6
- [7] Prateek Chhikara, Rajkumar Tekchandani, Neeraj Kumar, and Sudeep Tanwar. Federated learning-based aerial image segmentation for collision-free movement and landing. In *Proceedings of the 4th ACM MobiCom Workshop on Drone Assisted Wireless Communications for 5G and Beyond*, pages 13–18, 2021. 3
- [8] Jia Deng, Wei Dong, Richard Socher, Li-Jia Li, Kai Li, and Li Fei-Fei. Imagenet: A large-scale hierarchical image database. In *2009 IEEE Conference on Computer Vision and Pattern Recognition*, pages 248–255, 2009. 6
- [9] Jiahua Dong, Duzhen Zhang, Yang Cong, Wei Cong, Henghui Ding, and Dengxin Dai. Federated incremental semantic segmentation. In *Proceedings of the IEEE/CVF Conference on Computer Vision and Pattern Recognition (CVPR)*, pages 3934–3943, 2023. 2
- [10] Runmin Dong, Lichao Mou, Mengxuan Chen, Weijia Li, Xin-Yi Tong, Shuai Yuan, Lixian Zhang, Juepeng Zheng, Xiaoxiang Zhu, and Haohuan Fu. Large-scale land cover mapping with fine-grained classes via class-aware semi-supervised semantic segmentation. In *Proceedings of the IEEE/CVF International Conference on Computer Vision (ICCV)*, pages 16783–16793, 2023. 1, 2
- [11] Lidia Fantauzzo, Eros Fani, Debora Caldarola, Antonio Tavera, Fabio Cermelli, Marco Ciccone, and Barbara Caputo. Feddrive: Generalizing federated learning to semantic segmentation in autonomous driving. In *2022 IEEE/RSJ International Conference on Intelligent Robots and Systems (IROS)*, pages 11504–11511, 2022. 2
- [12] Michael F Goodchild. The validity and usefulness of laws in geographic information science and geography. *Annals of the Association of American Geographers*, 94(2):300–303, 2004. 2
- [13] Kaiming He, Xiangyu Zhang, Shaoqing Ren, and Jian Sun. Deep residual learning for image recognition. In *Proceedings of the IEEE Conference on Computer Vision and Pattern Recognition (CVPR)*, 2016. 6
- [14] Fan Huang, Sida Jiang, Wenfeng Zhan, Benjamin Bechtel, Zihan Liu, Matthias Demuzere, Yuan Huang, Yong Xu, Lei Ma, Wanjun Xia, et al. Mapping local climate zones for cities: A large review. *Remote Sensing of Environment*, 292: 113573, 2023. 2
- [15] Wei Huang, Chang Chen, Yong Li, Jiacheng Li, Cheng Li, Fenglong Song, Youliang Yan, and Zhiwei Xiong. Style projected clustering for domain generalized semantic segmentation. In *Proceedings of the IEEE/CVF Conference on Computer Vision and Pattern Recognition (CVPR)*, pages 3061–3071, 2023. 2
- [16] Wenke Huang, Mang Ye, Zekun Shi, He Li, and Bo Du. Rethinking federated learning with domain shift: A prototype view. In *Proceedings of the IEEE/CVF Conference on Computer Vision and Pattern Recognition (CVPR)*, pages 16312–16322, 2023. 3
- [17] Yash Khasgiwala, Dion Trevor Castellino, and Sujata Deshmukh. A decentralized federated learning paradigm for semantic segmentation of geospatial data. In *Intelligent Computing & Optimization: Proceedings of the 4th International Conference on Intelligent Computing and Optimization 2021 (ICO2021) 3*, pages 196–206. Springer, 2022. 3
- [18] Qinbin Li, Yiqun Diao, Quan Chen, and Bingsheng He. Federated learning on non-iid data silos: An experimental study. In *2022 IEEE 38th International Conference on Data Engineering (ICDE)*, pages 965–978, 2022. 2
- [19] Tian Li, Anit Kumar Sahu, Manzil Zaheer, Maziar Sanjabi, Ameet Talwalkar, and Virginia Smith. Federated optimization in heterogeneous networks. In *Proceedings of Machine Learning and Systems*, pages 429–450, 2020. 2, 6, 8
- [20] Zhuohong Li, Wei He, Mofan Cheng, Jingxin Hu, Guangyi Yang, and Hongyan Zhang. Sinolc-1: the first 1 m resolution national-scale land-cover map of china created with a deep learning framework and open-access data. *Earth System Science Data*, 15(11):4749–4780, 2023. 2
- [21] Quande Liu, Cheng Chen, Jing Qin, Qi Dou, and Pheng-Ann Heng. Feddg: Federated domain generalization on medical image segmentation via episodic learning in continuous frequency space. In *Proceedings of the IEEE/CVF Conference on Computer Vision and Pattern Recognition (CVPR)*, pages 1013–1023, 2021. 2
- [22] Songlin Liu, Linwei Chen, Li Zhang, Jun Hu, and Ying Fu. A large-scale climate-aware satellite image dataset for domain adaptive land-cover semantic segmentation. *ISPRS Journal of Photogrammetry and Remote Sensing*, 205:98–114, 2023. 5
- [23] Yi Liu, Jiangtian Nie, Xuandi Li, Syed Hassan Ahmed, Wei Yang Bryan Lim, and Chunyan Miao. Federated learning in

- the sky: Aerial-ground air quality sensing framework with uav swarms. *IEEE Internet of Things Journal*, 8(12):9827–9837, 2021. 3
- [24] Emmanuel Maggiori, Yuliya Tarabalka, Guillaume Charpiat, and Pierre Alliez. Can semantic labeling methods generalize to any city? the inria aerial image labeling benchmark. In *2017 IEEE International Geoscience and Remote Sensing Symposium (IGARSS)*, pages 3226–3229, 2017. 5
- [25] Brendan McMahan, Eider Moore, Daniel Ramage, Seth Hampson, and Blaise Aguera y Arcas. Communication-efficient learning of deep networks from decentralized data. In *Artificial intelligence and statistics*, pages 1273–1282. PMLR, 2017. 1, 2, 6, 8
- [26] Matias Mendieta, Taojiannan Yang, Pu Wang, Minwoo Lee, Zhengming Ding, and Chen Chen. Local learning matters: Rethinking data heterogeneity in federated learning. In *Proceedings of the IEEE/CVF Conference on Computer Vision and Pattern Recognition (CVPR)*, pages 8397–8406, 2022. 2
- [27] Jiaxu Miao, Zongxin Yang, Leilei Fan, and Yi Yang. Fedseg: Class-heterogeneous federated learning for semantic segmentation. In *Proceedings of the IEEE/CVF Conference on Computer Vision and Pattern Recognition (CVPR)*, pages 8042–8052, 2023. 2
- [28] Umberto Michieli, Marco Toldo, and Mete Ozay. Federated learning via attentive margin of semantic feature representations. *IEEE Internet of Things Journal*, 10(2):1517–1535, 2023. 3
- [29] Liangqiong Qu, Yuyin Zhou, Paul Pu Liang, Yingda Xia, Feifei Wang, Ehsan Adeli, Li Fei-Fei, and Daniel Rubin. Rethinking architecture design for tackling data heterogeneity in federated learning. In *Proceedings of the IEEE/CVF Conference on Computer Vision and Pattern Recognition (CVPR)*, pages 10061–10071, 2022. 3
- [30] Dario Schulz, He Yin, Bernhard Tischbein, Sarah Verleysdonk, Rabani Adamou, and Navneet Kumar. Land use mapping using sentinel-1 and sentinel-2 time series in a heterogeneous landscape in niger, sahel. *ISPRS Journal of Photogrammetry and Remote Sensing*, 178:97–111, 2021. 2
- [31] Xinyi Shang, Yang Lu, Gang Huang, and Hanzi Wang. Federated learning on heterogeneous and long-tailed data via classifier re-training with federated features. In *Proceedings of the Thirty-First International Joint Conference on Artificial Intelligence, IJCAI-22*, pages 2218–2224, 2022. 2, 6, 8
- [32] Mennatullah Siam, Boris N. Oreshkin, and Martin Jagersand. Amp: Adaptive masked proxies for few-shot segmentation. In *Proceedings of the IEEE/CVF International Conference on Computer Vision (ICCV)*, 2019. 5
- [33] Yafei Song and Ganggang Dong. Federated target recognition for multiradar sensor data security. *IEEE Transactions on Geoscience and Remote Sensing*, 61:1–10, 2023. 3
- [34] Prohim Tam, Sa Math, Chaebeen Nam, and Seokhoon Kim. Adaptive resource optimized edge federated learning in real-time image sensing classifications. *IEEE Journal of Selected Topics in Applied Earth Observations and Remote Sensing*, 14:10929–10940, 2021. 3
- [35] Haifa Tamiminia, Bahram Salehi, Masoud Mahdianpari, Lindi Quackenbush, Sarina Adeli, and Brian Brisco. Google earth engine for geo-big data applications: A meta-analysis and systematic review. *ISPRS Journal of Photogrammetry and Remote Sensing*, 164:152–170, 2020. 1
- [36] Aysim Toker, Lukas Kondmann, Mark Weber, Marvin Eisenberger, Andrés Camero, Jingliang Hu, Ariadna Pregel Hoderlein, Çağlar Şenaras, Timothy Davis, Daniel Cremers, Giovanni Marchisio, Xiao Xiang Zhu, and Laura Leal-Taixé. Dynamicearthnet: Daily multi-spectral satellite dataset for semantic change segmentation. In *Proceedings of the IEEE/CVF Conference on Computer Vision and Pattern Recognition (CVPR)*, pages 21158–21167, 2022. 2
- [37] Xin-Yi Tong, Gui-Song Xia, and Xiao Xiang Zhu. Enabling country-scale land cover mapping with meter-resolution satellite imagery. *ISPRS Journal of Photogrammetry and Remote Sensing*, 196:178–196, 2023. 1, 2, 5
- [38] Haozhao Wang, Yichen Li, Wenchao Xu, Ruixuan Li, Yufeng Zhan, and Zhigang Zeng. Dafkd: Domain-aware federated knowledge distillation. In *Proceedings of the IEEE/CVF Conference on Computer Vision and Pattern Recognition (CVPR)*, pages 20412–20421, 2023. 2
- [39] Jingdong Wang, Ke Sun, Tianheng Cheng, Borui Jiang, Chaorui Deng, Yang Zhao, Dong Liu, Yadong Mu, Mingkui Tan, Xinggang Wang, Wenyu Liu, and Bin Xiao. Deep high-resolution representation learning for visual recognition. *IEEE Transactions on Pattern Analysis and Machine Intelligence*, 43(10):3349–3364, 2021. 8
- [40] Jia-Wen Xiao, Chang-Bin Zhang, Jiekang Feng, Xialei Liu, Joost van de Weijer, and Ming-Ming Cheng. Endpoints weight fusion for class incremental semantic segmentation. In *Proceedings of the IEEE/CVF Conference on Computer Vision and Pattern Recognition (CVPR)*, pages 7204–7213, 2023. 5
- [41] Enze Xie, Wenhai Wang, Zhiding Yu, Anima Anandkumar, Jose M Alvarez, and Ping Luo. Segformer: Simple and efficient design for semantic segmentation with transformers. In *Neural Information Processing Systems (NeurIPS)*, 2021. 8
- [42] An Xu, Wenqi Li, Pengfei Guo, Dong Yang, Holger R. Roth, Ali Hatamizadeh, Can Zhao, Daguang Xu, Heng Huang, and Ziyue Xu. Closing the generalization gap of cross-silo federated medical image segmentation. In *Proceedings of the IEEE/CVF Conference on Computer Vision and Pattern Recognition (CVPR)*, pages 20866–20875, 2022. 6, 8
- [43] Yonghao Xu, Tao Bai, Weikang Yu, Shizhen Chang, Peter M. Atkinson, and Pedram Ghamisi. Ai security for geoscience and remote sensing: Challenges and future trends. *IEEE Geoscience and Remote Sensing Magazine*, 11(2):60–85, 2023. 1, 3
- [44] Qiang Yang, Yang Liu, Tianjian Chen, and Yongxin Tong. Federated machine learning: Concept and applications. *ACM Transactions on Intelligent Systems and Technology (TIST)*, 10(2):1–19, 2019. 1
- [45] Mang Ye, Xiuwen Fang, Bo Du, Pong C Yuen, and Dacheng Tao. Heterogeneous federated learning: State-of-the-art and research challenges. *ACM Computing Surveys*, 56(3):1–44, 2023. 2
- [46] Yaopei Zeng, Lei Liu, Li Liu, Li Shen, Shaoguo Liu, and Baoyuan Wu. Global balanced experts for federated long-

- tailed learning. In *Proceedings of the IEEE/CVF International Conference on Computer Vision (ICCV)*, pages 4815–4825, 2023. [2](#)
- [47] Boning Zhang, Xiaokang Zhang, Man-On Pun, and Ming Liu. Prototype-based clustered federated learning for semantic segmentation of aerial images. In *IGARSS 2022 - 2022 IEEE International Geoscience and Remote Sensing Symposium*, pages 2227–2230, 2022. [3](#)
- [48] Xiaokang Zhang, Boning Zhang, Weikang Yu, and Xudong Kang. Federated deep learning with prototype matching for object extraction from very-high-resolution remote sensing images. *IEEE Transactions on Geoscience and Remote Sensing*, 61:1–16, 2023. [3](#)
- [49] Yifan Zhang, Bingyi Kang, Bryan Hooi, Shuicheng Yan, and Jiashi Feng. Deep long-tailed learning: A survey. *IEEE Transactions on Pattern Analysis and Machine Intelligence*, 45(9):10795–10816, 2023. [2](#)
- [50] Zheng Zhang, Xindi Ma, and Jianfeng Ma. Local differential privacy based membership-privacy-preserving federated learning for deep-learning-driven remote sensing. *Remote Sensing*, 15(20):5050, 2023. [3](#)
- [51] Zhijia Zheng, Shihong Du, Yi-Chen Wang, and Qiao Wang. Mining the regularity of landscape-structure heterogeneity to improve urban land-cover mapping. *Remote Sensing of Environment*, 214:14–32, 2018. [2](#)
- [52] Yanfei Zhong, Bowen Yan, Jingjun Yi, Ruiyi Yang, Mengzi Xu, Yu Su, Zhendong Zheng, and Liangpei Zhang. Global urban high-resolution land-use mapping: From benchmarks to multi-megacity applications. *Remote Sensing of Environment*, 298:113758, 2023. [1](#), [2](#)

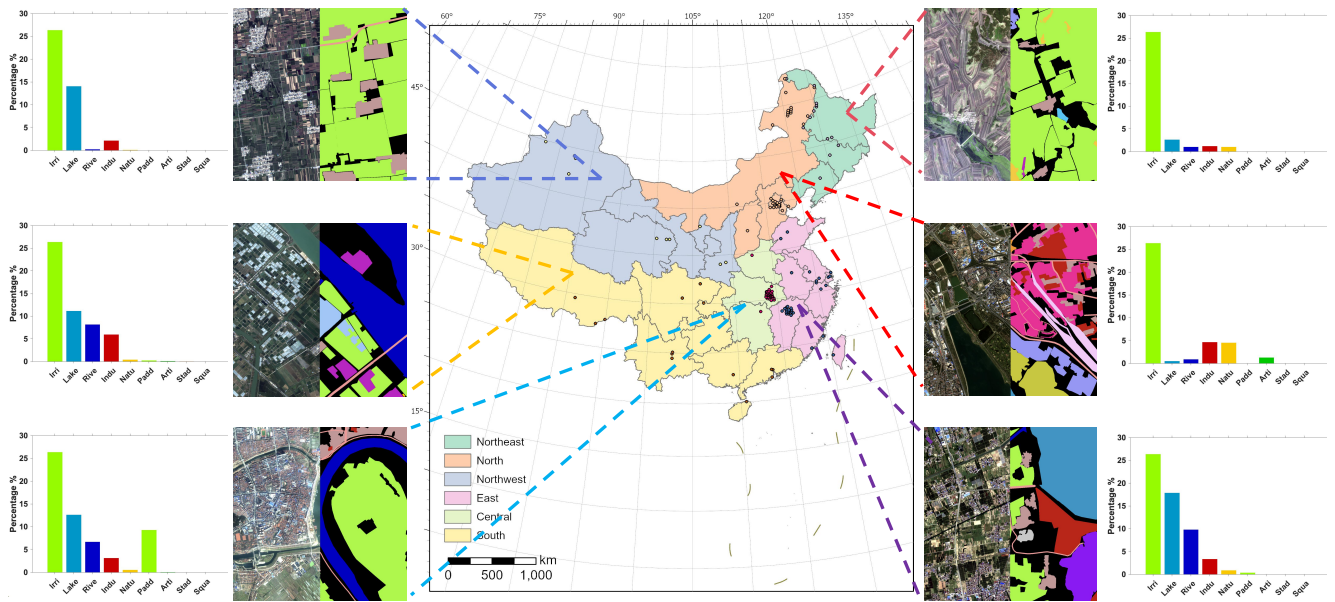


Figure 7. Geographic heterogeneity in FBP dataset.

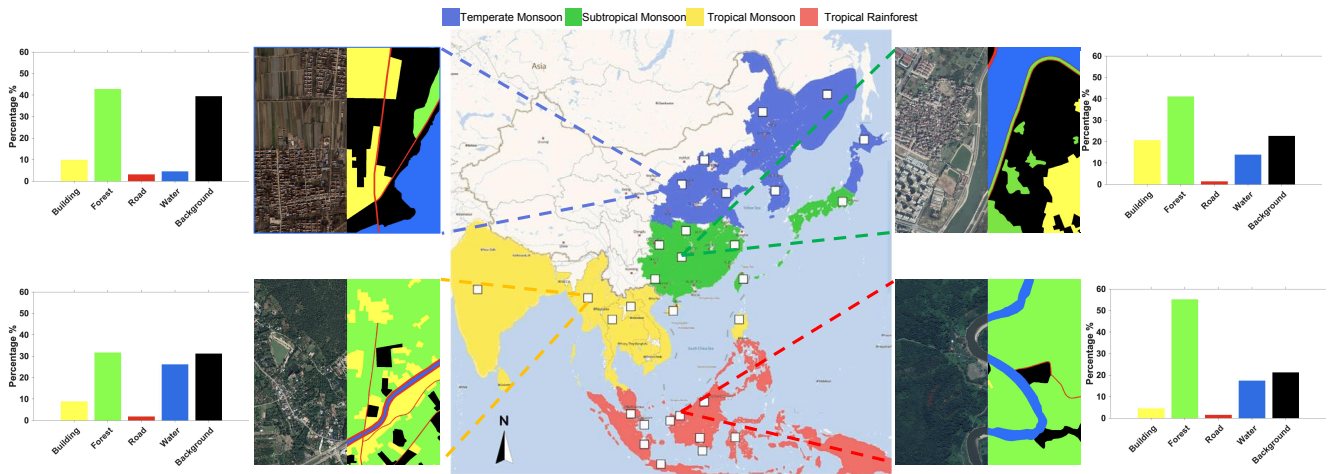


Figure 8. Geographic heterogeneity in CASID dataset.

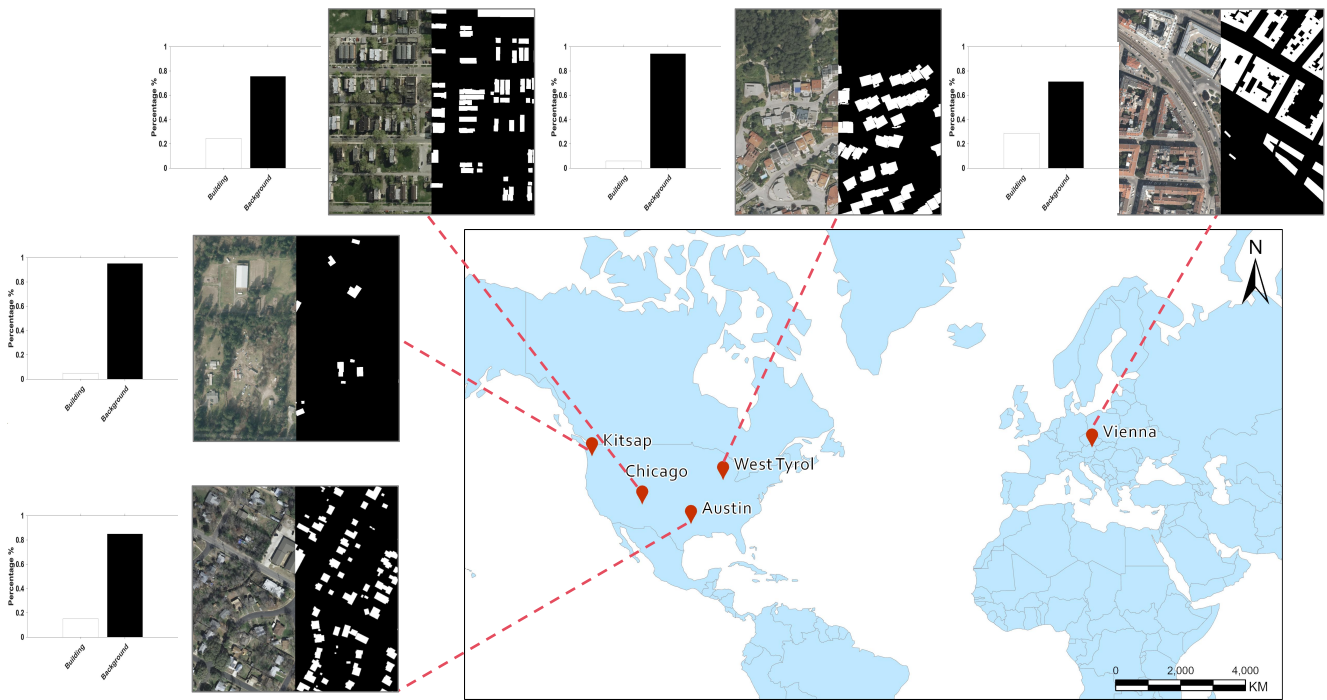


Figure 9. Geographic heterogeneity in Inria dataset.